Journal of the European Ceramic Society **7** (1991) 227–236

Uniaxial Tension and Cyclic Tension–Compression Testing of Ceramics

J. N. Adami, D. Bolsch,* J. Bressers,‡ E. Fenske & M. Steen

Institute for Advanced Materials, Joint Research Centre, CEC, P.O. Box 2, 1755 ZG Petten, The Netherlands

(Received 27 August 1990; accepted 5 November 1990)

Abstract

Two loading and gripping systems for the uniaxial testing of ceramics in tension–creep and in cyclic tension–compression respectively, are presented. In both systems flat samples are held in hydraulic grips (cold gripping). The tensile set-up incorporates an adjustable universal joint in the loading train in order to minimize the bending level in the specimens. Low bending in the rigid, cyclic tension–compression set-up is achieved by appropriate alignment of the loading train–grip assembly prior to the onset of a test series.

The relevant quantity to characterize the alignment performance of a loading train–grip assembly is the maximum *level of bending along the gauge length of a uniaxial specimen, expressed in terms of the precision of alignment P. The correct procedure to measure this* maximum *is reiterated. The* maximum *precision of alignment which is achieved at the failure stresses of the materials under investigation is smaller than approximately* $4{\cdot}5 \times 10^{-5}$ *and* $3{\cdot}5 \times 10^{-5}$ *in the tension and cyclic tension–compression systems, respectively.*

Für die uniaxiale Prüfung keramischer Werkstoffe werden zwei Einspann- und Belastungssysteme für Zug–Kriechversuche und für Zug–Druck–Wechselversuche vorgestellt. In beiden Systemen werden die Flachproben mit einer hydraulischen Klemmung eingespannt (kalte Einspannung). Mit dem Ziel die unerwünschte Biegung in den Proben zu minimieren, ist in der Zug–Kriechvorrichtung ein justierbares Kreuzgelenk eingebaut. Niedrige Biegungswerte in der steifen Zug–Druck–Wechselvorrichtung werden durch geeignete Ausrichtung der Klemmvorrichtung und Lastkette vor dem Beginn einer Versuchsreihe erreicht.

Massgebend für die Charakterisierung der vorliegenden Ausrichtungsfähigkeit ist die maximal *vorhandene Biegung bezogen auf die Messlänge der Probe. Sie wird als Präzision P der Ausrichtung bezeichnet. Die Bestimmung dieses* Maximums *wird nochmals beschrieben. Für die untersuchten Materialien wird eine* maximale *Präzision der Ausrichtung P zum Zeitpunkt des Versagens besser als* $4{\cdot}5 \times 10^{-5}$ *für die Zug–Kriech- und* $3{\cdot}5 \times 10^{-5}$ *für die Zug–Druck–Wechselbelastungsvorrichtung erreicht.*

On présente ici deux systèmes de chargement et de serrage pour essais uniaxiaux sur céramiques, respectivement en traction–fluage et en traction–compression cyclique. Dans les deux systèmes les échantillons sont maintenus par des mors hydrauliques (serrage à froid). Le montage de traction incorpore un joint universel réglable dans le train de charge qui a pour but de minimiser le niveau de flexion dans les échantillons. Dans le montage rigide pour traction–compression cyclique, on obtient des flexions faibles en alignant convenablement l'assemblage mors–train de charge avant le début d'une série d'essais.

Le paramètre caractérisant la qualité de l'alignement d'un assemblage mors–train de charge est le niveau de flexion maximum *dans la longueur étalonnée d'un échantillon uniaxial, exprimée en termes de précision d'alignement P. Le mode opératoire correct afin de déterminer ce* maximum *est repris. La précision* maximale *de l'alignement atteinte à la contrainte de rupture des matériaux testés est inférieure à* $4{\cdot}5 \times 10^{-5}$ *pour le système de traction et à* $3{\cdot}5 \times 10^{-5}$ *pour le système de traction–compression cyclique.*

* Present address: Deutsche Airbus, P.O. Box 1120, D-2874 Lemwerder, FRG.
‡ To whom correspondence should be addressed.

1 Introduction

Traditionally, ceramics are tested in flexure for the purpose of characterizing their mechanical behaviour and generating design databases. However, the flexure test has two major drawbacks.[1] At low-to-intermediate temperatures the failure strength of ceramics is controlled by the stress necessary to propagate a critical flaw to failure. The measured failure strength depends on the volume fraction of the specimen or component subjected to the maximum stress because of the increasing probability of the presence of a critical 'defect–stress' combination in increasingly larger volumes. The very small volume probed at the maximum stress in a flexure test therefore limits the usefulness of flexure data for design-oriented databases. The inhomogeneity of the stress field in a flexure sample and the resulting stress redistribution during plastic deformation or creep[1] constitutes the other major drawback of flexure testing. Asymmetric deformation[1] in the tension and compression parts of the flexure samples obscures the interpretation of stress-dependent damage and fracture mechanisms under high-temperature loading. The uniaxial, tensile-type of test, on the other hand, offers the advantages of a uniform and well-defined stress field in time and in space, and of a relatively large tested volume.

The major difficulty associated with the uniaxial test is the achievement of a uniform stress distribution through an optimal alignment of the loading train, grips and specimen assembly. Indeed, even a small misalignment can cause noticeable effects on the test result when the extent of plasticity in the test is small. This can be due to the confinement of the plastic deformation to a small fraction of the test piece (as in notched sample testing), to the regime of deformation studied (microyield measurements) or simply to the inherent brittleness of the material (for a review see Ref. 2). In ceramics, low-temperature tests are most sensitive to non-uniform stress distributions in view of their restricted plasticity.

Excellent analyses of the alignment problem in uniaxial tension and creep testing are given in the literature by Schmieder[3] and by Christ & Swanson.[4] Measures and techniques to overcome misalignment are reviewed by Bressers.[2] For the tensile testing of ceramics various gripping systems are reported in the literature.[5–18] With the exception of the oil-bearing systems,[10,18] the solutions proposed during the 1980s to minimize the misalignment in the testing of ceramics are based on the gripping systems advocated earlier for the purpose of obtaining good alignment in uniaxial testing in general. The percentage bending (PB) levels reported for the testing of ceramics range from $PB \leq 5\%$ to $PB \leq 2\%$.[5–18] For the oil-bearing systems the inventors claim bending levels $PB \leq 0{\cdot}5$–1%.[10,18] Cyclic testing, in particular tension–compression fatigue in the uniaxial mode, presents an even greater challenge and it is scarcely reported upon in the literature.[16,17,19–21] Bending levels of $PB \sim 5\%$ are quoted by authors using non-adjustable grips,[16,17,19] and bending levels of $PB < 1\%$ to $PB < 3\%$ in tension and compression, respectively, with adjustable grips.[20,21]

In this paper two loading and gripping concepts for the uniaxial testing of ceramics in tension–creep and in cyclic tension–compression, respectively, are presented. The performance of both systems in terms of their potential for alignment is assessed and discussed. The analysis of bending in the two systems is used to formulate recommendations with respect to the adequate measurement and reporting of alignment data in uniaxial ceramics testing.

2 Definitions

When a ceramic specimen is loaded uniaxially during, say, a tensile test, the force acting in any cross-section of the gauge length is generally not constant over the whole area, i.e. the stress state is not ideally uniaxial. The inherent brittleness of the ceramic material precludes stress redistribution during the tensile test, so that a local peak stress is soon reached and, in the presence of a critical Griffith flaw, the failure criterion is met. In a linear elastic hypothesis, assuming that any cross-section remains plane during deformation, the strains measured in that cross-section on two opposite locations of the specimen perimeter are not equal (Fig. 1). The percentage bending in the corresponding direction is defined as half the difference of the strains ε_1 and ε_2, which represents the bending strain ε_b, divided by the average strain ε_0:[3,4]

$$PB = 100 \cdot \varepsilon_b / \varepsilon_0 \tag{1}$$

where

$$\varepsilon_b = |(\varepsilon_1 - \varepsilon_2)|/2$$

and

$$\varepsilon_0 = (\varepsilon_1 + \varepsilon_2)/2$$

According to this definition, the PB decreases with increasing load, when it is assumed that the bending strains remain constant during loading. This dependence has caused some confusion amongst

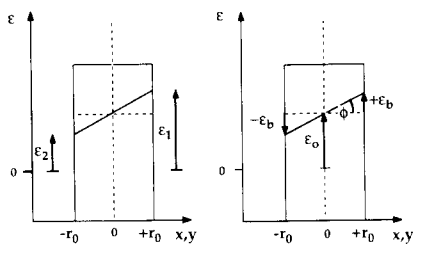

Fig. 1. Measured strains ε_1 and ε_2 on two opposite sides of a specimen under uniaxial load F (a) and definition of the average strain ε_0 and the bending strain ε_b in two perpendicular directions x and y (b).

scientists when comparing alignment data, which certainly negatively affects the standardization efforts in this field. Another way of quantifying bending strains is through the precision of alignment P, which is based on the angle ϕ between the longitudinal axis of the specimen and the normal to the cross-section after deformation (see Fig. 1):

$$\tan \phi = |\varepsilon_b| l_0 / r_0 \qquad (2)$$

where r_0 is half the distance between the corresponding strain measurement positions and l_0 is the measuring length. Under the same assumptions as before, the precision of alignment does not depend on the load level and thus provides a better assessment of the quality of alignment. It is worth noting that the minimum of P corresponds to the maximum level of alignment.

These definitions are based on the measurement of the bending strains on the surface of the specimen, ideally by means of strain gauges. They apply equally well to specimens having rectangular or circular cross-sections. The direction of measurement, however, does not necessarily coincide with the direction of the local maximum of the bending strain in the cross-section under consideration. In order to determine this local maximum, four strain gauges are glued on the perimeter in two perpendicular directions x and y corresponding to the axes of symmetry of the section, see Fig. 2. The resulting bending strains ε_{bx}, ε_{by} (i.e. ε_b in the x and y directions, respectively) represent the components of the bending strain vector **B** which characterizes the angular position and the magnitude of the maximum bending strain in that section.

Thus

$$\mathbf{B}_i = \begin{bmatrix} B_{x,i} \\ B_{y,i} \end{bmatrix} = \begin{bmatrix} \varepsilon_{bx,i} \\ \varepsilon_{by,i} \end{bmatrix}$$

where the index i ($=1, 2, 3$) stands for the cross-section considered. Rigorously speaking, only the

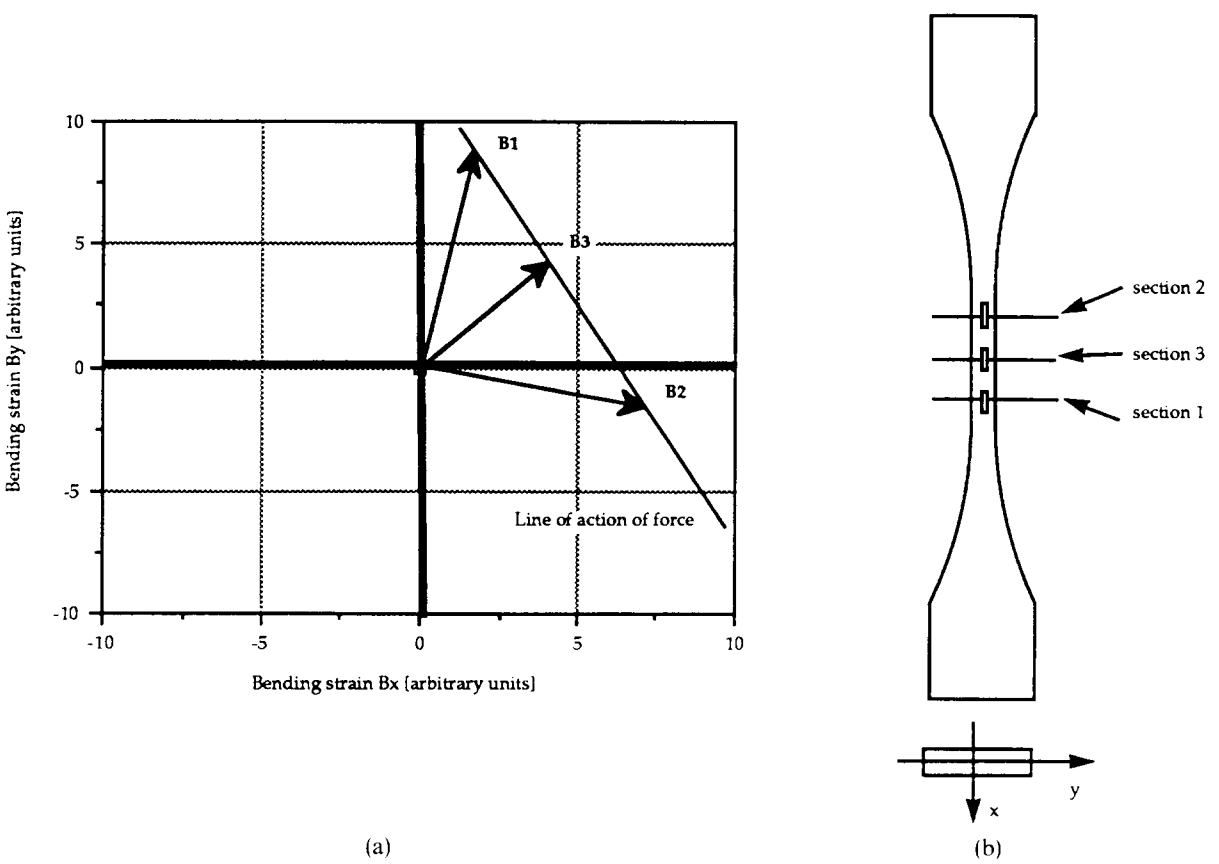

Fig. 2. Representation of the **B** vector in the planes (B_x, B_y) (a) of three equispaced cross-sections 1, 2 and 3 of the tensile sample (b) where the strain gauges are positioned.

maximum value of the **B** vector along the specimen gauge length has to be considered when discussing alignment. The geometrical locus of the extremities of all the **B** vectors along the specimen gauge length is defined as the line of action of force (see Fig. 2). The *maximum* value of the **B** vector along the gauge length is easily determined from the line of action of force.

3 Experimental Procedure

The test specimens are flat, dog-bone shaped samples with a parallel gauge length of 30 mm and a rectangular cross-section of $6 \times 8\,mm^2$. The dimensions of the cross-sections at the gripping ends are $6 \times 20\,mm^2$ or $6 \times 24\,mm^2$. Account is taken of the volume effect in optimizing the ratio of the two cross-sections. One of the main advantages of the flat specimen geometry is that the effect of machining can be minimized by grinding parallel to the loading direction as opposed to the situation in circumferentially machined cylindrical specimens. All the specimens are tested in the as-machined condition, without chamfered edges. Evidence of failures starting preferentially from the edges is not observed. In order to restrict the contribution of the specimen to the overall bending, the samples are machined to close tolerances, in particular with regard to plane parallellism: $2\,\mu m$ and $4\,\mu m$ along the specimen thickness and along the two width dimensions (cross-section and clamping ends), respectively. Two different monolithic ceramic materials have been tested under uniaxial tensile conditions: alumina (22 specimens) and zirconia (24 specimens). The material used in the tension–compression tests is a hot-pressed silicon nitride (27 specimens).

The alignment performance of the two loading and gripping systems is measured on two accurately aligned testing machines. A 100 kN electro-mechanical Schenck-Trebel testing machine and a 100 kN hydraulic Schenck testing machine are used for tension and cyclic tension–compression testing, respectively. The load train configuration for both monotonic and cyclic uniaxial tests includes a pair of MTS 646.10 hydraulic grips equipped with flat 6×24 mm collets. These allow both a repeatable mounting of the specimen as well as a fine adjustment of the clamping pressure applied to the specimen ends. In both set-ups the lower grip is fixed rigidly to the machine and aligned according to the procedure described later. In the tensile test configuration a modified universal joint is added between the top grip and the load cell. This device allows self-adjusting of angularity errors and provides manual correction possibilities for eccentricity errors. The function of the universal joint is to compensate for the misalignment due to inaccurate clamping of the specimen in the grips. The alignment procedure consists of adjusting the position of the top grip until the minimum of the **B** vector in the cross-sections considered is found. Only one universal joint is included in the load train, since experience has shown that with two joints (situated below the lower and above the upper grip, respectively) the small improvement in alignment that can be obtained at low stress levels tends to be lost as soon as the load is increased.

In the tension–compression set-up similar hydraulic grips as described above are used. In the case of through-zero cycling it is impossible to incorporate a universal joint in the load train since it behaves mechanically unstable in compression. Consequently a rigid load train has to be used. In order to compensate for angularity errors in this case, both rams connecting the grips to the testing machine are shimmed. For this, it is necessary to load the testing machine using a metallic sample of large cross-section clamped into the grips, then to place the shim(s) at the correct angular position, preload the load train with the spiral washers, remove the metal sample and check for parallelism using a dial gauge displaced along the grip. Eccentricity errors are minimized by careful machining and assembling of the constituent parts of the loading and gripping system. The quality of the alignment therefore relies entirely upon a perfect shimming of the rams, a highly reproducible clamping, as well as close dimensional tolerances of all constituent parts of the load train and of the specimen.

Bending strains are measured on two perimeters located at 10 mm off the centre position of the gauge length, using four strain gauges in each cross-section. In some experiments 12 strain gauges, equispaced on three cross-sections, are used, see Fig. 2. The reference measurement for the strain gauges is made at zero load with only one end of the specimen clamped in the grips. Subsequently the other end is clamped, and the strain gauge readings as well as the load are recorded and stored via a Hewlett-Packard 3852A data acquisition unit in a Macintosh II using LabVIEW software. Because of the high sampling rate as well as computing capability of this combination, the bending strains can be monitored in real time and the **B** vector in each of the cross-sections can be visualized on the screen. The displayed values are updated approximately every 2 s. On-line monitoring of the **B** vector

offers the possibility for interactive optimization. The alignment is first optimized at a low stress level of 20 MPa in the manner described later. Subsequently the applied load is increased continuously up to approximately 100 MPa and the evolution of the bending strains with applied load is recorded. For the tension–compression tests the same procedure is applied in compression as well. Subsequently the load is brought back to near-zero level and the specimen is either tested to fracture at a constant load rate or subjected to a load controlled cyclic fatigue test. In some tensile tests, the bending strains have been recorded up to failure of the specimen.

The two systems are successfully used for the uniaxial testing of monolithic ceramics and ceramic matrix composites in tension and creep, and in cyclic tension–compression up to temperatures of 1450°C. Since only the specimen is heated and the grips are water-cooled, the alignment of the systems is not affected by a change in temperature of the specimen.

4 Results and Discussion

4.1 Tensile test set-up

Figure 3 shows the end points of the **B** vector (the origin coincides with the origin of the coordinate system) in the two outer cross-sections 1 and 2 (see Fig. 2) at the alignment stress level of 20 MPa for both materials. With a few exceptions, the absolute values $|B_x|$ and $|B_y|$ of the components of the **B** vector are smaller than 5 microstrain. Figure 3 refers to alignment results obtained using a single universal joint. When two joints are used, comparable results are obtained. The magnitude of the B vector in section 1 (largest distance from the universal joint) is

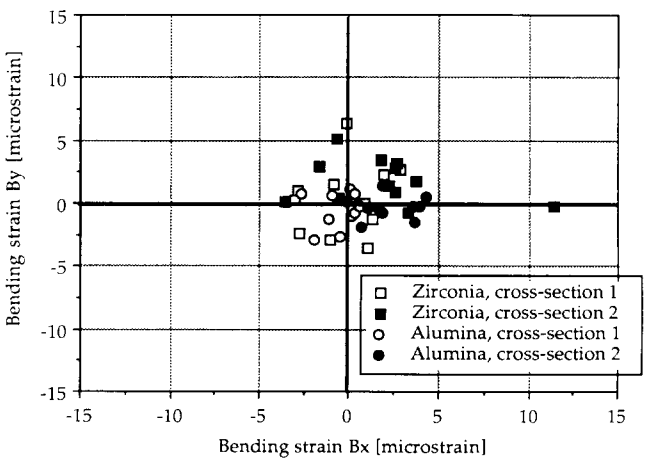

Fig. 3. Alumina and zirconia **B** vectors at the alignment stress (20 MPa) for the tensile set-up.

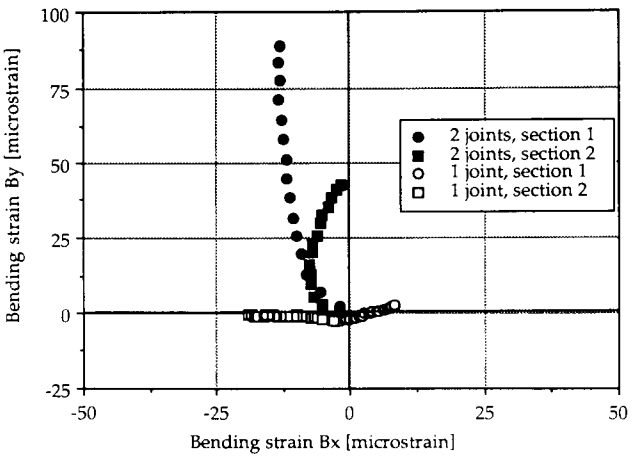

Fig. 4. Evolution of the **B** vector in two zirconia samples in two cross-sections during a tensile test up to 160 MPa.

generally smaller than the level of bending in section 2 (nearest to the joint).

The changes of the **B** vector in both magnitude and direction upon increasing the load level from the alignment stress to the failure stress are plotted in Fig. 4 for the two outer cross-sections of two zirconia specimens, for the single- and for the double-joint set-ups, respectively. Although comparable levels of bending are obtained at the alignment stress level of 20 MPa, the bending level increases much more sharply in the double-joint set-up.

The data for the single-joint set-up are represented in a different way in Fig. 5. During loading the x-component and to a smaller extent also the y-component of the **B** vector in both sections is observed to increase in absolute value from its minimum value achieved at the alignment stress. The directional change of the **B** vector provoked by increasing the stress level from the alignment stress

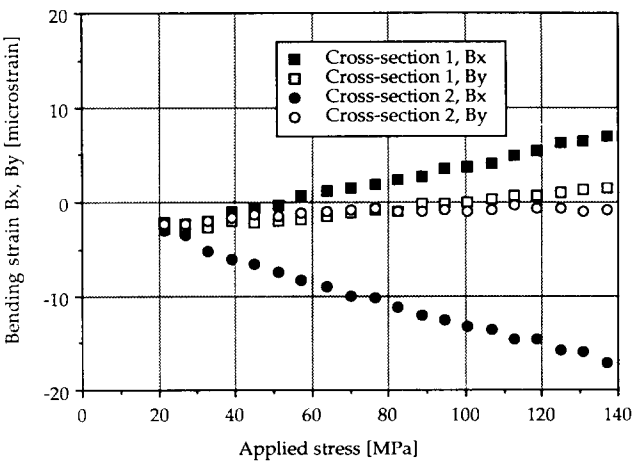

Fig. 5. Evolution of the **B** vector coordinates versus applied stress for a zirconia specimen using the tensile set-up.

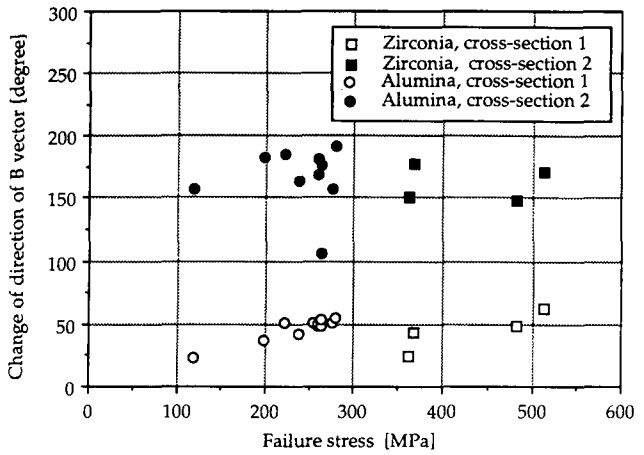

Fig. 6. Change of direction of the **B** vector between alignment and failure stress levels for the tensile set-up.

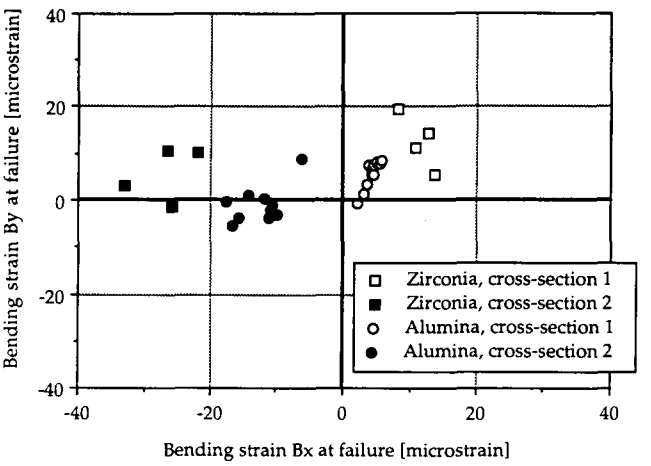

Fig. 8. Alumina and zirconia **B** vectors at the failure stresses for the tensile set-up.

to the failure stress is shown in Fig. 6 as a function of the failure stress for the case of the single-joint set-up. The plot includes all the results where failure occurred within the gauge length. The directional change is virtually independent of the applied stress. The change in length of the **B** vector with loading from the alignment stress to the failure stress, on the other hand, is load dependent, as shown in Fig. 7.

The performance of the single-joint tensile set-up is illustrated in Fig. 8 in terms of the **B** vector length at failure. Because of the higher failure stress, the increase in **B** vector with increasing stress is largest for zirconia. The **B** vector lengths in section 2 (nearest to the joint) increase more sharply and move in an opposite direction relative to those in section 1. Finally, the x-components of the **B** vector tend to be larger than the y-components, as opposed to the case at the alignment stress level.

The *maximum* bending along the gauge length can be derived when the line of action of force is known. Figure 9 shows the **B** vectors $\mathbf{B}_1$ and $\mathbf{B}_2$ in the two outer cross-sections 1 and 2 for the zirconia tensile specimen with the largest *PB* at failure. Assuming a linear line of action of force, the length of the **B** vector in the centre cross-section, $\mathbf{B}_3$, equals the average of $\mathbf{B}_1$ and $\mathbf{B}_2$. The corresponding calculated value of *PB* in the centre cross-section is then 0·87%. The *maximum PB* along the gauge length is 2·5%, which is approximately three times the bending at the centre cross-section. This finding emphasizes that it is necessary to determine the **B** vector in at least two cross-sections to be able to find its maximum (and thus also the maximum *PB*) along the gauge length. Conversely, it is shown that strain measurements performed in the centre cross-section only, result in an unconservative estimate of the maximum *PB* level along the gauge length.

In Fig. 10(a) and (b) the range of the *maximum* percentage bending and of the corresponding *maximum* precision of alignment, respectively, are plotted versus the applied stress. These ranges encompass bending results of all the alumina and

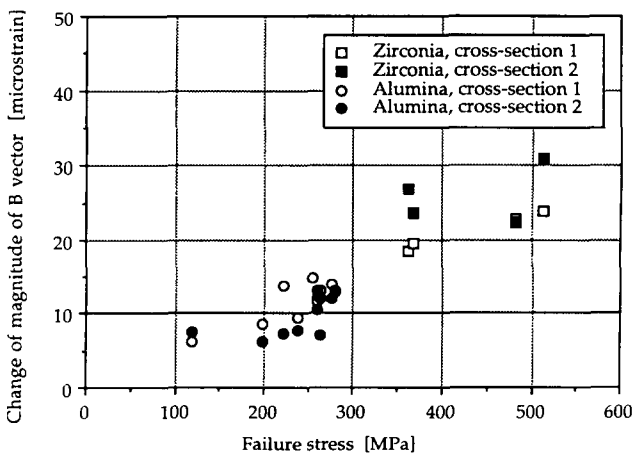

Fig. 7. Change of magnitude of the **B** vector between alignment and failure stress levels for the tensile set-up.

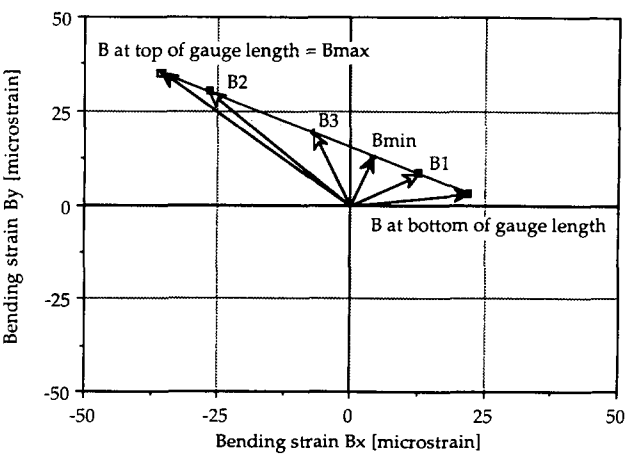

Fig. 9. Line of action of force and determination of *maximum* **B** vector in the tensile specimen with the largest bending.

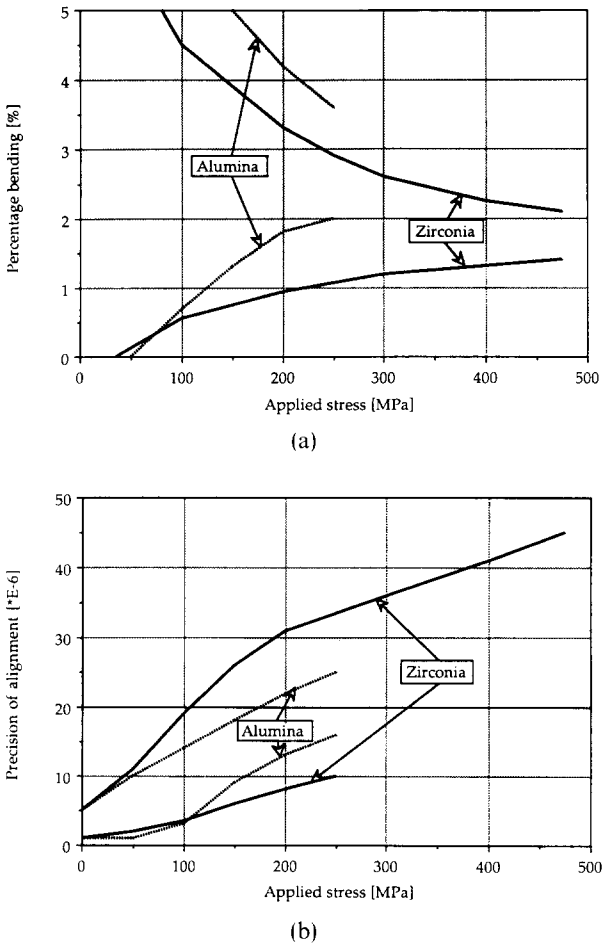

Fig. 10. Range of (a) *maximum* percentage bending and (b) *maximum* precision of alignment versus applied stress for all samples tested in the tensile set-up.

zirconia samples. At failure the *maximum* percentage bending and the *maximum* precision of alignment for alumina and zirconia achieved with the tensile set-up are, respectively:

$$PB < 3{\cdot}5\% \quad \text{and} \quad P < 2{\cdot}5 \times 10^{-5} \quad \text{for alumina}$$
$$PB < 2{\cdot}5\% \quad \text{and} \quad P < 4{\cdot}5 \times 10^{-5} \quad \text{for zirconia}$$

The ratio of the *maximum PB* (or *maximum P*) along the gauge length to the *PB* (or *P*) in the centre cross-section varies between approximately 3 and 6.

Hence in the centre cross-section:

$$PB < 1\% \quad \text{and} \quad P < 1{\cdot}5 \times 10^{-5}$$

4.2 Tension–compression set-up

Figure 11 shows the end points of the **B** vector obtained with the tension–compression set-up using an alumina specimen loaded from 10 to 100 MPa. As opposed to the tensile set-up, the **B** vectors in both sections remain more stable over this stress range, both in direction and in length. However, they are larger in magnitude than in the case of the tensile set-up.

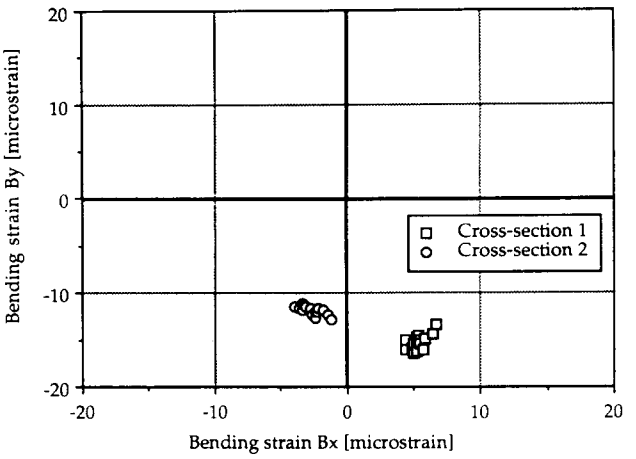

Fig. 11. Evolution of the **B** vector for an alumina specimen using the tension–compression set-up.

Figure 12 shows the evolution of the **B** vector components with stress for the same test. They remain constant over the whole stress range, and their level depends on the original alignment achieved on the set-up rather than on clamping or specimen geometry induced misalignment. As shown earlier in Fig. 5, this is not the case for the tensile set-up, where the components of the **B** vector gradually increase from a small optimum value at the alignment stress onwards. Although the tensile set-up thus shows better alignment capability at low stresses, there is a stress level at which the bending strains using this set-up will be higher than in the tension–compression set-up. Whether this cross-over will effectively be reached depends on the strength of the material tested.

Figure 13 shows the alignment results at 80 ± 5 MPa for HPSN samples tested on the tension–compression set-up along with alumina and zirconia test results obtained on the tensile set-up. The

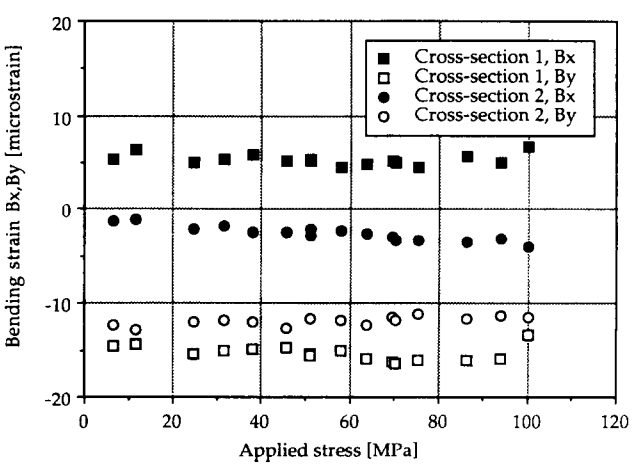

Fig. 12. Evolution of the **B** vector coordinates versus applied stress for an alumina specimen using the tension–compression set-up.

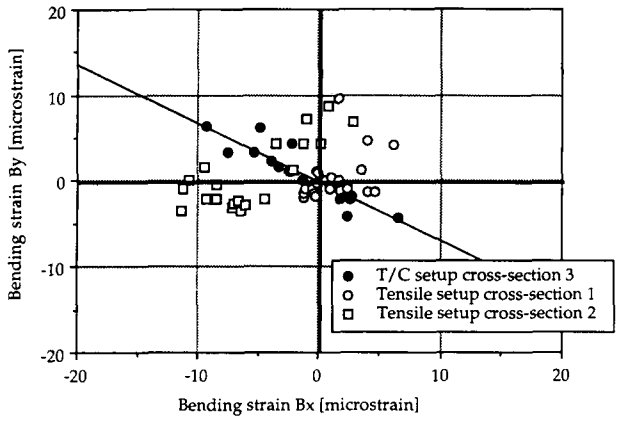

Fig. 13. Alignment results of both set-ups: **B** vector at 80 ± 5 MPa in alumina, zirconia and HPSN specimens.

tension–compression set-up results are clustered along a straight line, and not randomly spaced about the origin. This is caused by the permanent misalignment introduced during assembly of the rigid load train. The advantage of the suggested representation is that it gives a qualitative indication about where the shims must be placed to improve alignment. The only way of reducing the area covered by the **B** vector in Fig. 13 is to realign the load train.

The *maximum* precision of alignment which can be achieved in the tension–compression set-up is illustrated in Fig. 14 for a series of specimens. In all cases the *maximum P* is smaller than $3{\cdot}5 \times 10^{-5}$, corresponding to *maximum* percentage bending levels at failure of $PB < 1\%$, $PB < 2{\cdot}4\%$ and $PB < 0{\cdot}8\%$ for HPSN, alumina and zirconia, respectively. In the centre cross-section $P < 1{\cdot}5 \times 10^{-5}$, leading to a percentage bending level $PB < 1\%$ for all materials.

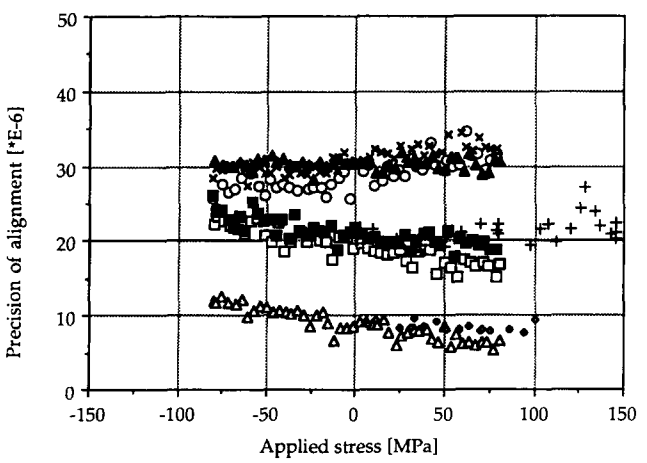

Fig. 14. *Maximum* precision of alignment versus applied stress for a series of samples tested in the tension–compression set-up. Each sample is represented by a different symbol.

5 Performance and Recommendations

The definition of the maximum allowable bending, or of the minimum required precision of alignment in a test depends on, amongst other factors, the effect of the bending level on the property measured in that test. Because this effect is seldom quantified one has to resort to other means in order to judge upon the performance of a uniaxial testing system. An indirect route is to correlate the position of *maximum* bending along the gauge length with the failure location. Figure 15 shows a histogram of the failure locations along the gauge length of the specimens. As can be observed, 50 specimens out of a total of 73 (46 under monotonic and 27 under cyclic loading) fail in the gauge length portion without any preference for failure to occur near either end of the gauge length where the *maximum* bending occurs. It thus appears that the precision of alignment achieved in both systems is below the limit beyond which bending would obscure the intrinsic failure characteristics of the materials tested under the given loading conditions.

The relevant quantity when assessing the alignment performance of a uniaxial testing system is the *maximum* bending occurring along the gauge length. The bending strains in at least two perimeters along the gauge length need to be measured in order to enable the line of action of force and, hence, the *maximum* bending to be determined, assuming elastic deformation of the specimen. The bending levels quoted in the literature[5–21] for the various tension and tension–compression loading and gripping systems are, with a very few exceptions, measured in only one perimeter, usually at the centre of the gauge length. For the vast majority of the samples tested the ratio between these two bending

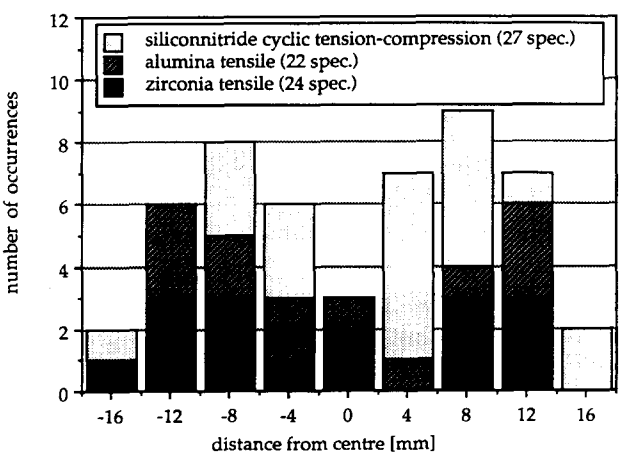

Fig. 15. Failure location for all valid test results on alumina, zirconia and HPSN specimens.

levels ranges from 3 to 6 in the tensile set-up and from 2 to 3 in the tension–compression set-up. The bending level in the centre of the gauge length hence gives a misleading impression of the alignment performance of a uniaxial testing system.

The lack of a standard procedure for measuring and reporting the quality of alignment thus precludes the assessment and the comparison of the alignment performances of the uniaxial loading and gripping systems quoted in the literature. Expressing the quality of alignment in terms of the percentage bending at a specific but arbitrarily chosen stress further contributes to the confusion. The present authors therefore recommend the use of the precision of alignment P for quantifying the alignment performance. In a rigid system the quality of alignment of the loading train and grips is fully characterized by a single value of P over the entire load range. The presence of a universal joint in the loading train may cause P to change with increasing stress. It is then recommended that P values are reported for the stress associated with the mechanical property under investigation; for example, for the range of fracture stresses in a series of strength tests, or for the range of creep stresses applied in a creep testing programme, etc.

6 Conclusions

Two loading and gripping systems, conceived for the uniaxial testing of ceramics in tension–creep and in cyclic tension–compression, respectively, are described and assessed in terms of their alignment performance. The assessment is based on bending measurements performed on a total of 73 specimens of alumina, zirconia and HPSN.

It is recommended that the quality of alignment of a uniaxial testing system is expressed in terms of the precision of alignment P rather than in terms of the percentage bending PB which is the quantity invariably reported in the literature. It is also recommended that P values are reported at the stress level associated with the phenomenon under investigation.

Bending data quoted in the literature refer nearly always to the level of bending in the centre cross-section of the specimens' gauge length. Because the ratio between the *maximum* bending and the bending in the centre cross-section can take on relatively large values and even increase to infinity in the case of equal but opposite eccentricities at each end of the gauge length, centre-of-gauge-length bending levels are misleading. The relevant quantity to quantify the quality of alignment is the *maximum* bending along the gauge length.

The tensile set-up, which contains a universal joint, enables a *maximum* precision of alignment $P < 4{\cdot}5 \times 10^{-5}$ over the stress range up to 450 MPa, corresponding to *maximum* percentage bending levels at failure of $PB < 3{\cdot}5\%$ and $PB < 2{\cdot}5\%$ for alumina and zirconia, respectively. In the rigid tension–compression set-up the *maximum* precision is $P < 3{\cdot}5 \times 10^{-5}$ independent of the stress, corresponding to *maximum* percentage bending levels at failure of $PB < 2{\cdot}4\%$ for alumina and $PB < 1\%$ for zirconia and HPSN. The corresponding levels of bending at the centre of the gauge length are $P < 1{\cdot}5 \times 10^{-5}$ and $PB < 1\%$ at the failure stresses of all the samples tested. This quality of alignment is at the better end of the range of alignment performances of uniaxial testing systems proposed in the literature.

Acknowledgements

The authors gratefully acknowledge Messrs G. Bracke, G. von Birgelen and C. Bobeldijk for their assistance and Hoogovens for the use of their alumina and zirconia specimens.

References

1. Gratwohl, G., Current testing methods—a critical assessment. *Int. J. High Technol. Ceram.*, **4** (1988) 123–42.
2. Bressers, J., Axiality of loading. In *Measurement of High Temperature Mechanical Properties of Materials*, ed. M. S. Loveday, M. F. Day & B. F. Dyson. HMSO, London, 1982, pp. 278–95.
3. Schmieder, A. K., Measuring the apparatus contribution to bending in tension specimens. In *Elevated Temperature Testing Problem Areas*. ASTM STP 488, 1970, pp. 15–42.
4. Christ, B. W. & Swanson, S. R., Alignment problems in the tensile test. *J. Test. Evaluation*, **4** (1971) 405–17.
5. Davies, C. K. L. & Sinha Ray, S. K., A simple apparatus for carrying out tensile creep tests on brittle materials up to temperatures of 1750°C. *J. Physics E.: Scientific Instruments*, **4** (1971) 421–4.
6. Lange, F. F. & Diaz, E. S., Powder-cushion gripping to promote good alignment in tensile testing. *J. Test. Evaluation*, **6** (1978) 320–3.
7. Govila, R. K., High-temperature uniaxial tensile stress rupture strength of sintered α-SiC. *J. Mat. Sci.*, **18** (1983) 1967–76.
8. Soma, T., Matsui, M. & Oda, I., Tensile strength of a sintered silicon nitride. In *Non-Oxide Technical and Engineering Ceramics*, ed. S. Hampshire. Elsevier Applied Science, London, 1985, pp. 361–79.
9. Liu, K. C. & Brinkman, C. R., Tensile cyclic fatigue of structural ceramics. In *Proceedings 23rd Automotive Technology Development Contractors' Coordination Meeting*, P-165, SAE, 1985, pp. 279–84.
10. Seshadri, S. G. & Kai-Yin Chia, Tensile testing of ceramics. *J. Am. Ceram. Soc.*, **70** (1987) C-242–4.

11. Ohji, T., Sakai, S., Ito, M., Yamauchi, Y., Kanematsu, W. & Ito, S., Tensile strength properties of hot-pressed silicon nitride. In *Proceedings 30th Japanese Congress on Materials Research*. The Society of Materials Science, Japan, 1987, pp. 201–6.
12. Carroll, D. F. & Wiederhorn, S. M., High-temperature creep testing of ceramics. *Int. J. High Technol. Ceram.*, **4** (1988) 227–41.
13. Kandil, F. A. & Dyson, B. F., Tensile creep of ceramics: the development of a testing facility. *Int. J. High Technol. Ceram.*, **4** (1988) 243–62.
14. Hermansson, T. & Dunlop, G. L., A high-temperature tensile testing rig for ceramic materials. *Int. J. High Technol. Ceram.*, **4** (1988) 263–8.
15. Essam, G. R. & Syers, G., Novel test methods for mechanical strength characterisation of engineering ceramics. *Int. J. High Technol. Ceram.*, **4** (1988) 275–80.
16. Soma, T., Masuda, M., Matsui, M. & Oda, I., Cyclic fatigue testing of ceramic materials. *Int. J. High Technol. Ceram.*, **4** (1988) 289–99.
17. Gürtler, M., Weddigen, A. & Gratwohl, G., Werkstoffprüfung von Hochleistungskeramik mit Zugproben. *Mat. Wiss. u. Werkstofftech.*, **20** (1989) 291–9.
18. Larsen, C. G., Ceramics Tensile Grip, MTS Systems Corporation, personal communication, 1989.
19. Guiu, F., Cyclic fatigue of polycrystalline alumina in direct push–pull. *J. Mat. Sci.*, **13** (1978) 1357–61.
20. Nitta, A., Ogata, T. & Fugioka, T., Evaluation tests of SiC ceramics fracture strength under tension–compression cyclic loading at ultra-high temperatures. In *Proceedings 25th Symposium on Strength of Materials at High Temperature*. The Society of Materials Science, Japan, 1987, pp. 137–41.
21. Amaral, J. E. & Pollock, C. N., Machine design requirements for uniaxial testing of ceramics materials. *Int. J. High Technol. Ceram.*, **4** (1988) 143–60.